ELSEVIER

Polymer 40 (1998) 53–64

polymer

Thermally crosslinkable thermoplastic PET-co-XTA copolyesters

Elizabeth Pingel[a], Larry J. Markoski[b], Gary E. Spilman[c], Brendan J. Foran[d], Tao Jiang[e], David C. Martin[e,*]

[a]*Dow Corning, Inc., Midland, MI, USA*
[b]*University of Illinois, Urbana, IL, USA*
[c]*General Electric Plastics, Mt. Vernon, IN, USA*
[d]*Sematech, Inc. Austin, TX, USA*
[e]*The Macromolecular Science and Engineering Center and the Materials Science and Engineering Department, The University of Michigan, 2022 H. H. Dow Building, Ann Arbor, MI 48109-2136, USA*

Received 27 November 1997; revised 9 February 1998; accepted 5 March 1998

Abstract

A series of thermally crosslinkable polyester copolymers were synthesized by incorporation of a benzocyclobutene-containing terephthalic acid derivative (XTA) into polyethylene terephthalate (PET). The cyclobutene moiety on the XTA monomer allows for reactive crosslinking at temperatures ~350°C requiring no catalyst and causing no change in mass. Copolymers were synthesized containing 1, 5, 10, 20, 50, and 100 mol% XTA. Crosslinking occurred above the melting temperature (~250°C) yet below the degradation temperature (~400°C), providing a window for melt processing of the copolymer. To demonstrate this point fibres were melt spun. The PET-co-XTA copolymers show systematic variations in the glass transition, recrystallization, melting and degradation temperatures as a function of benzocyclobutene content. The degradation and melting temperature both decrease slightly with increased XTA, while the recrystallization and glass transition temperature were relatively insensitive to XTA content. Thermal gravimetric analysis (TGA) indicated a decrease in the degradation temperature as higher amounts of XTA were incorporated, although an increase in the %char at 800°C was seen. This decrease in degradation temperature may be due to the generation of free radicals. Limiting Oxygen Index (LOI) measurements showed an increase in the oxygen content required to maintain a stable flame in copolymers with increasing amounts of XTA. LOI values ranged from 18 for neat PET to 35 for the copolymer containing 20 mol % XTA. Wide-angle X-ray scattering data showed little change in the crystalline structure, but decreasing crystallinity for PET for blends containing up to 20 mol% XTA. The 50 mol% XTA copolymer was amorphous, while the 100% XTA homopolymer (PEXTA) showed evidence of a new crystalline structure. Crystalline diffraction peaks showed reduced intensities in data recorded for heat treated samples, and there was evidence for new peaks in the copolymer containing 20 mol% XTA when heated near 300°C. Transmission electron microscopy of cross-sections through burned samples showed a highly crystalline char at the surface of XTA copolyesters. This crystalline char appeared to protect the underlying copolymer from further flame-induced degradation. Evidence for significantly increased adhesion of the copolymers to polyimide films was also obtained.

Keywords: Poly(ethylene terephthalate) (PET); Benzocyclobutane; Flame retardance

1. Introduction

Poly(ethylene terephthalate) (PET) is a high volume, commodity thermoplastic used in bottles, films, strapping, and flexible packaging [1]. In this paper we report the synthesis and characterization of copolymers of PET with a benzocyclobutene (BCB) functionalized, thermally crosslinkable variant of terephthalic acid, 1,2-dihydrocyclobutabenzene 3,6 dicarboxylic acid, (termed XTA) as shown in Fig. 1. In previous work it was shown that XTA could be effectively incorporated into many different types of high performance polymers to provide an additional means of control over materials properties [2–8]. By varying the amount of BCB it is possible to vary the concentration of crosslinks and therefore tailor the functionality of the copolymers to meet specific needs. Spilman discussed the effects of incorporation of BCB-containing monomers into several commercially important polymers including poly(*p*-phenyleneterephthalamide) (Kevlar®), polybenzobisthiazoles, poly (hydroxybenzoic acid-napthoic acid) (HBA/HNA) (Vectra®), and poly(*m*-phenylenediamine isophthalamide) (Nomex®) [8]. Some of the properties which were enhanced by crosslinking include solvent resistance, creep resistance, and flame resistance.

* Corresponding author.

0032-3861/98/$ - see front matter
PII: S0032-3861(98)00216-X

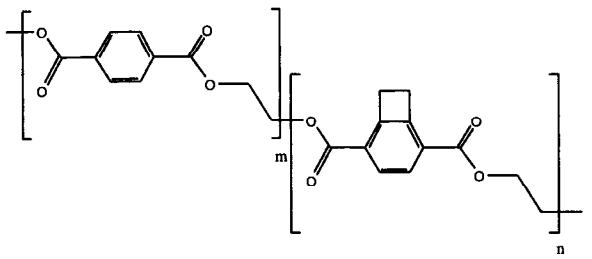

Fig. 1. Chemical structure of the PET-co-XTA copolymers.

One goal of this work was to investigate the hypothesis that copolymerization with the XTA monomer would improve the flame resistance of PET. In this introduction we first discuss the design of flame-resistant polymers in order to illustrate how BCB functional groups might be effective in this regard. We then discuss previous work on benzocyclobutene functionalized polymers before proceeding with the experimental protocol, results and discussion, and finally our conclusions.

1.1. Polymer flammability and flame resistance

The combustion of polymeric materials accounts for 94% of lives lost and 80% of reported injuries occurring in fires [9]. Flame retardants are thus of considerable interest. Additives should work at low concentrations, be easily incorporated into materials, have little effect on processing and physical properties, and also be cost-effective [10]. Flame retardants must break the cycle of combustion by either removing heat that causes degradation, decreasing the release of volatile components, scavenging the oxidative free radicals, or insulating the unburned material from the flame [11,12].

Polymers including many polyimides, aromatic polyamides (i.e., Nomex®), polybenzimidazole, stepladder polypyrrolones, and polyquinoxalines have been specifically developed to be thermally stable, but these are generally expensive and thus tend to be limited to specialty applications. For less expensive commodity polymers better flame resistance is acquired through interrupting either the vapour phase or solid phase burning processes by adding vapour phase inhibitors such as halogen- and phosphorus-containing compounds (as well as synergysts like SbO_3) that scavenge free radicals

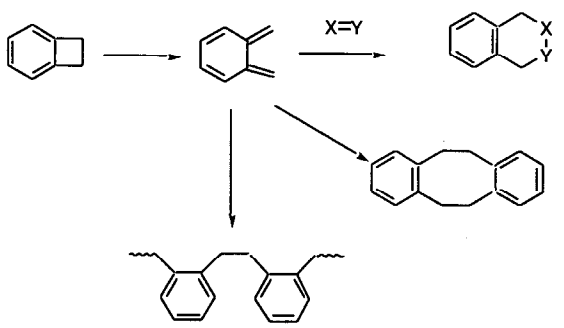

Fig. 2. A schematic of the possible reaction pathways for BCB [16].

involved in the oxidation process [13]. Halogen-based flame retardants such as polybrominated diphenyl ethers are environmentally hazardous as they may release HCl and HBr on combustion [13].

Intumescent coatings work on the concept of solid phase inhibition by generating noncombustible gases and forming rigid carbonaceous surface char layers which protect the underlying polymer [10]. A problem with this method is that if the coating is compromised there is nothing in the polymer itself to stop the flame. Filler materials such as silica, and calcium carbonate, have been used to decrease flammability by acting as heat sinks, but high loadings are usually required to obtain significant decreases in flammability and this tends to adversely affect physical properties [10,11,13]. Incorporation of crosslinking agents into the polymer backbone can provide a means of char layer formation and crosslinking may also slow the flow of unburned polymer that is required to fuel the flame front [11].

1.2. Benzocyclobutene chemistry

Kirchhoff et al. [14] and Kirchoff and Bruza [15] have reviewed the synthetic schemes and polymerizations of many types of BCB-containing monomers, and the analysis of materials properties of the resulting polymers. Farona has also recently discussed new advances in the area of BCB polymer chemistry, including polymers containing more than one BCB group [15]. BCB end-capped polymers and oligomers can react to provide chain extension, branching and crosslinking. Potential applications include biocompatibilized materials, fibres, coatings and films for microelectronics, and high performance polymers. The BCB moiety consists of a four-membered ring which may thermally rearrange to form an *o*-quinodimethane derivative, which may then react with another ring-opened BCB group to polymerize forming a poly(*o*-xylylene) or, when a suitable dienophile is present, react through a Diels–Alder mechanism (see Fig. 2) [14–16]. Reactions between two BCB groups (avg. $\Delta H = -53 \pm 3$ kcal) as well as between a BCB group and a site of unsaturation (avg. $\Delta H = -44 \pm 3$ kcal) were determined to be thermodynamically favoured. The Diels–Alder pathway was reported as kinetically preferred [14,15].

Kirchhoff et al. developed a variety of monomers with amide, aryl, ester, aliphatic, and unsaturated linkages between BCB end-groups [14,15]. The thermal stability of the polymers ranged from 365 to 475°C, and was not correlated to the degree of aryl content. The ethylene-linked material had the highest thermal stability, indicative that the linkage groups participated in the homopolymerization reactions. Graft copolymers have been produced with BCB chemistry through the Diels–Alder mechanism. In these systems BCB end-capped graft segments may react with ethylene linkages or with other BCB groups. For example, polyarylate segments were grafted onto EPDM rubber using BCBs [16]. Also BCB end-capped polystyrene segments

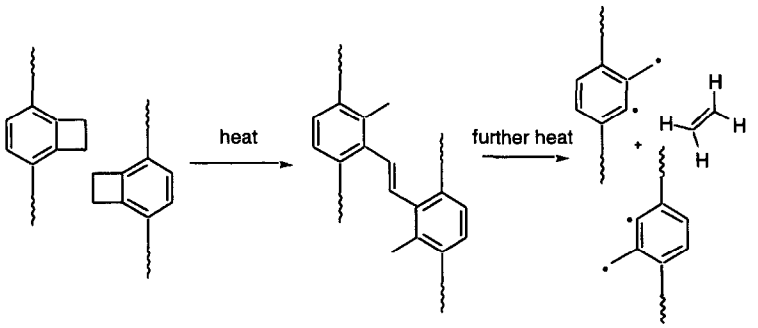

Fig. 3. Potential mechanism for the crosslinking and subsequent degradation of BCB crosslinks.

were grafted to poly-1-hexene-co-7-methyl-1,6-octadiene [17].

BCB chemistry has been used to introduce chain extension and branching in polystyrene. Most commercial polystyrene synthetic procedures use free radical polymerization. Introducing branching into the polymer tends to lead to gel formation within the reactors. A latent functional group was needed to branch the polymer after synthesis. BCB groups were introduced as a part of the initiator and mostly attached as end groups to the polymer chain. Heating at 240°C caused the molecular weight of the polymer to increase up to 4 times its original weight. This was attributed to cycloaddition reactions between the BCB groups [18].

BCBs were used as thermal crosslinking agents in curing procedures of 1,1′-(methylene di-4,1-phenylene)bismaleimides (BMI) [19,20]. An improved thermo-oxidative stability was observed for the BCB–BMI polymers. For 200 h at 343°C in air, the cured BMI maintained only 3% of its initial weight, while all mixtures of BCB–BMI showed a 13–15% weight loss [19,20]. Several BCB-terminated aromatic imide monomers and oligomers were synthesized and subsequently cured. The BCB-cured polymers showed only a 17% weight loss after 200 h at 316°C [19,20].

Grafting BCB groups onto olefinic polymers has been used to control the amount of crosslinking and long chain branching in those systems [21]. Low levels of crosslinking caused improved processability and improved optical and physical and mechanical properties. The olefinic polymers with BCB grafts can be blended with a wide variety of other polymers. Pendant BCB groups can compatibilize blends by reacting with sites of unsaturation or with other BCB groups. Acylation or alkylation of BCB groups onto various engineering thermoplastics has also allowed similar results [22]. BCB crosslinked polymers have shown improved solvent resistance and increased T_g.

BCB-terminated bisphenol A polycarbonate oligomers were also shown to crosslink into network polymers with improved solvent and ignition resistance, good toughness and improved surface hardness [23]. A drawback was that the thermo-oxidative stability decreased (indicated by the dark colours of the samples exposed to air at high temperatures) and the degradation temperature decreased proportionally with increasing BCB. The ductility went from high to low with increasing BCB content. Good solvents for bisphenol A polycarbonates, such as CH_2Cl_2 and THF, only swelled the BCB PCs, while other organic solvents swelled the BCB PCs with no measurable soluble fraction. The limiting oxygen index (LOI) of regular polycarbonate was 27 while that of the BCB terminated polymers was 42, a significant increase. Also the UL-94 rating increased from V-0 to V-2. The scratch hardness increased from 3B for the BPA PC to H for the BCB PC.

1.3. XTA monomer

Several polymer systems containing the XTA monomer have been studied to determine the effect of the BCB group on processing, crystallization, and other physical properties [2,4,5]. XTA incorporation into poly(*p*-phenyleneterephthalamide) (PPTA or Kevlar®) provided enhanced materials properties [4]. PPTA-co-XTA copolymer fibres were dry-jet wet spun from sulfuric acid solutions. Exothermic crosslinking occurred between 300 and 425°C with 380°C. Increases in the tensile modulus and tensile strength were found with higher annealing temperatures, although the toughness of the fibres decreased. A decrease in the tensile strength and fracture toughness after further heating was rationalized by thermal degradation occurring above the crosslinking temperatures.

BCB-modified polybenzobisthiazoles (PBZT) were synthesized and dry-jet wet spun [24]. Oriented fibres of the BCB-PBZT homopolymer and copolymer (75/25) were heat treated at 450°C and 330°C, respectively. The BCB-PBZT fibre heat-treated at 330°C showed a compressive strength of 0.48 GPa, which was about twice as high as the value for unmodified PBZT fibres. On the other hand, heat treatment at 450°C gave a compressive strength of 0.10 GPa, which was lower than the unmodified fibres. Through TGA/MS it was discovered that ethylene was liberated between 330 and 600°C with a maximum at 420°C, coinciding with the BCB crosslinking exotherm seen in the DSC. This indicated that bond breaking was occurring either as the crosslinks are forming or shortly thereafter. A proposed mechanism for this process is shown in Fig. 3.

ESR studies done on PPXTA showed the formation of

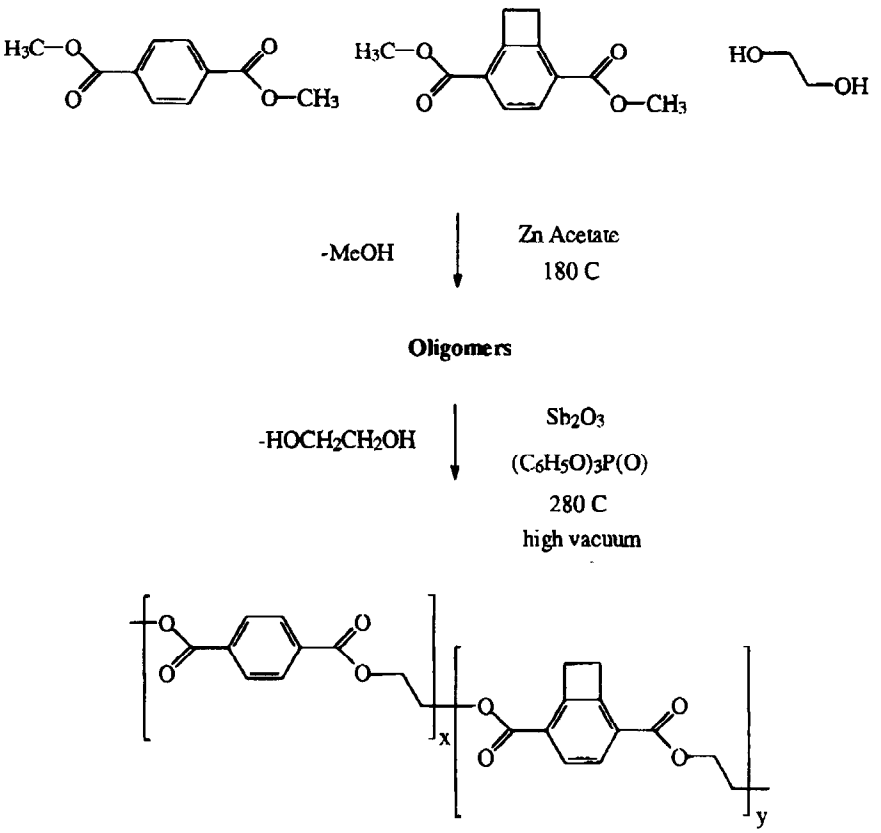

Fig. 4. Synthetic scheme for PET-co-XTA copolymers.

radicals (in air) after heat treatment at 380°C for 1 min [25]. The radicals persisted even when sitting at room temperature after heat treatment. It was determined that oxidation was responsible for the radical signal. This was confirmed by heating PPXTA under vacuum for 4 h at 380°C and no radical signal was seen. The degradation mechanism proposed in Fig. 3 is consistent with observations of the oxidative degradation of PPTA-co-XTA by Mielewski et al. [24].

BCB copolymers of thermotropic liquid crystalline polymers (TLCP) still formed mesophases and could be melt processed near 280°C before crosslinking at higher temperatures [5]. Increased XTA content caused a decrease in the onset of thermal degradation, from 505 to 450°C for HBA/HNA-co-20XTA, but the char yield at 900°C increased from 32.7% to 39.3%.

Copolymers of poly(*m*-phenylenediamine isophthalamide) (MPDI or Nomex®) with XTA showed thermal crosslinking from 382 to 405°C, a decrease in degradation temperature and a slight decrease in % residue at 800°C [8]. Fibres spun from the MPDI-co-XTA copolymers had greater dimensional stability in high heat compared with fibres made from neat MPDI. However, LOI data indicated either no change or a slight decrease in flame resistance with incorporation of the XTA monomer. This is evidently due to the fact that the MPDI polymers do not exhibit a stable melt phase before thermal degradation.

BCB moieties were incorporated into the polymer backbone of poly(arylene ether ketones), using the XTA monomer to provide increased materials processability and allow thermal crosslinking to form a stable insoluble network [26]. XTA crosslinked polyarylates based on fluorene bisphenol and *t*-butyl isophthalic acid dichloride showed a small increase in the gas permeability and a small decrease in the permselectivity, which was explained on the basis of degradation occurring at the high crosslinking temperatures [27].

2. Experimental

The XTA diester monomer was synthesized using established procedures [2,8]. PET and PET-co-XTA copolymers were synthesized by melt transesterification. Ethylene glycol (1.29 mol, 80.07 g), dimethyl terephthalate (0.522 mol, 101.37 g), and zinc acetate catalyst (2.6×10^{-4} mol, 0.057 g) (all from Aldrich) were combined and heated to 180°C, stirring with a Caframo, high torque motor with a stainless steel stirring shaft. As the reaction proceeded, methanol was released. An aspirator vacuum was used to facilitate its removal. The first step generally took about 3 h to complete. At this point the reacting mixture was clear. After a stoichiometric amount of methanol was removed antimony trioxide (2.3×10^{-4} mol, 0.067 g) and triphenyl

phosphate (2.2×10^{-4} mol, 0.072 g) were added to the system, along with several millilitres of ethylene glycol to wash them into the reaction vessel. The temperature was increased to 280°C. Ethylene glycol was removed from 240°C up to 280°C with an aspirator vacuum at first, then with a higher vacuum (approx. 200 mmHg) to remove the remainder [28]. If the molecular weight was not high enough the polymer was heated to melting under a higher vacuum (approx. 60 mm Hg) with a dry ice trap. Once the polymer reached a high molecular weight, the viscosity rose and the colour was slightly yellow.

To make PET-co-XTA copolymers the only change in procedure was to add XTA monomer at specific concentrations. Maintaining the reaction temperature below 280°C was critical to avoid BCB crosslinking. The PET-co-XTA polymers had a green tint which increased in intensity with XTA content. The synthetic scheme is shown in Fig. 4.

Wide-angle X-ray scattering was recorded on a Rigaku θ-2θ theta diffractometer with a 12 kW rotating anode source, monochromated Cu Kα radiation, $\lambda = 1.542$ Å in reflection mode. Hot-stage optical microscopy was performed on a Nikon Optiphot-POL equipped with a Linkham LH 1600 hot stage, video overlay system, and Macintosh Quadra computer with RasterOps Video board. The images were processed and analysed using Adobe Photoshop and NIH Image software. Ultraviolet spectroscopy was performed with a Perkin-Elmer u.v. Spectrometer. Transmission electron microscopy (TEM) (200 kV JEOL 2000 FX and 400 kV JEOL 4000 EX) was done on ~60 nm thin sections (Riechert-Jung ultramicrotome with DDK diamond knife) of burned copolymer embedded in epoxy (Pelco Eponate-12 from Ted Pella Inc.).

Viscosity measurements were done with a Cannon 50 E264 viscometer at 25°C in *o*-chlorophenol. The intrinsic viscosity was calculated by plotting specific viscosity versus concentration and extrapolating to zero. Molecular weights for PET were determined by using the Mark–Houwink equation, $[\eta] = kM^a$ (with $k = 6.56 \times 10^{-4}$ and $a = 0.73$) [29]. Estimates of the molecular weights for the copolymers were obtained by assuming that the as yet undetermined Mark–Houwink parameters were the same as for neat PET.

Table 1
Summary of viscosity and molecular weight data for PET-co-XTA

Compound	Viscosity (dl/g)	Estimated molecular weight (g/mol)
PET (neat)	0.52	9400
PET-co-XTA 1%	0.48	8400
PET-co-XTA 5%	0.47	8200
PET-co-XTA 10%	0.25	3400
PET-co-XTA 20%	0.23	3100
PET-co-XTA 50%	0.1	1000
PEXTA 100%	N/A	N/A

Thermal data were obtained from a Perkin-Elmer 7 series differential scanning calorimeter (DSC) and thermal gravimetric analyser (TGA). DSC data were obtained under nitrogen using a heating rate of 10°C/min from 25°C to approx. 400°C. TGA data were obtained in nitrogen and air with a heating rate of 40°C/min from 30 to 900°C and 10°C/min from 30 to 900°C. The data were analysed using the Perkin-Elmer 7 Series/UNIX Thermal Analysis System software provided with the system.

LOI data were obtained with an Atlas Limiting Oxygen Index chamber following standard ASTM D 2863 procedures. The test determines the minimum oxygen concentration in air necessary to support a stable flame. 1.3 mm × 6.5 mm × 8.1 cm samples for LOI testing were compression molded with a Tetrahedron hot press at 280°C for 5–10 min, then cooled to room temperature at a rate of 22.2°C/min with an applied force of 10 000 lbs.

Fibres were melt spun using a Bradford University Research Ltd. laboratory scale extruder through a 250 mm diameter spinnerette at temperatures ~10–20°C below the melting point of each copolymer. Solvent swelling experiments were performed by placing samples into *o*-chlorophenol. Crosslinked samples for these experiments were heated to 310°C for 10 min in a Lindburg tube furnace under a N_2 environment.

3. Results and discussion

3.1. Viscosity and molecular weight

A summary of the viscosity and molecular weight data is shown in Table 1. As the XTA content increased, the molecular weight of the polymers decreased. This could be attributed to the competing processes of crosslinking versus chain extension during the final stages of the synthesis. Although the molecular weights were fairly low, fibres could still be melt spun for all the samples except the 50% PET-co-XTA and the PEXTA 100%. The intrinsic viscosity for the PEXTA 100% was not obtained because it was not fully soluble in *o*-chlorophenol.

3.2. Hot-stage optical microscopy and u.v. spectroscopy

Samples melted repeatedly when heated to only 10°C above the melting point; the melt was clear and relatively colourless (Fig. 5). On cooling, the materials recrystallized with a slight brownish colour. Heating near crosslinking temperatures caused an increased greenish tint, while heating further resulted in orange–brown colouring. As evidence of crosslinking, the polymer would no longer recrystallize on cooling or flow when subsequently reheated (Fig. 5). The crosslinked polymers were found to be insoluble in the *o*-chlorophenol solvent.

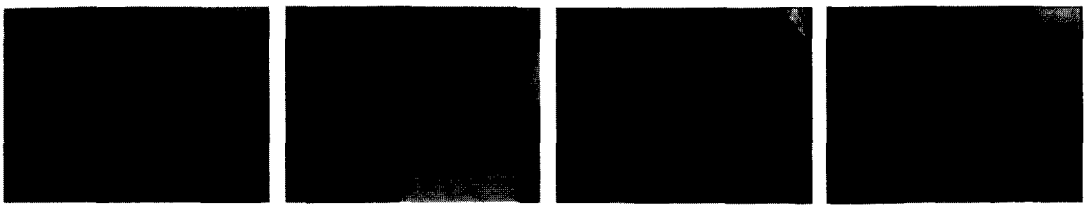

Fig. 5. Selected images from hot-stage optical microscopy of PET-co-XTA 4.8%. (a) First melting when heated to 260°C. (b) Cooled and fractured when solidified at room temperature. (c) Second melt showing flow. (d) Heated further to 350°C. The sample has now crosslinked into a rigid solid, and there was no additional flow observed in subsequent heating cycles.

The change in appearance was quantified by u.v. spectroscopy, where there was an increase in absorption seen near 500 nm after heat treatment of the BCB-containing copolymers (Fig. 6). This observation is consistent with the formation of extended conjugation between aromatic rings, providing further support for the stilbene bridge mechanism of crosslinking (Fig. 3). Since these sp^2-hybridized carbon bridges correspond to the repeat unit of polyparaphenylene (PPV), this result suggests that there may be future interest for the use of BCB functionalized molecules in applications which exploit this extended conjugation, such as in optoelectronically active devices.

3.3. Thermal characterization

The melting point (T_m), glass transition temperature (T_g), recrystallization temperature (T_{recry}) and the BCB crosslinking temperature (T_{rxn}) were obtained from DSC plots. A summary of the data can be found in Fig. 7, in which the characteristic temperatures are shown as a function of copolymer composition. T_g increased from 63 to 82°C from 0 to 5% XTA. At increasing concentrations of XTA T_g decreased. The 100% PEXTA had no observable T_g. A recrystallization peak was seen up through the 20 mol% PET-co-XTA. It gradually increased from 125°C (plain PET) to 137°C (PET-co-XTA 20%). There was a noticeable decrease to 122°C for the 10% PET-co-XTA. The melting points of the PET-co-XTA copolymers steadily decreased as XTA content increased, though a slight initial increase from 0 to 1% PET-co-XTA was seen. At 50 mol% no melting point was observed, indicating very little or no crystallinity. The 100% PEXTA had a melting point (255°C) which happened to be comparable with the neat PET (247°C).

BCB crosslinking was not observed for the 1 and 5% PET-co-XTA in the DSC. This may be due to a small reaction DH which could not to be detected. The BCB crosslinking temperature for the 10 and 20% PET-co-XTA was observed at ~370°C. The crosslinking temperatures of the 50% and 100% copolymers were not clearly resolved. This may be due to the crosslinking temperatures occurring very close to the degradation temperatures. If degradation started to occur within the DSC, the samples appeared gelled and were very difficult to remove from the sample pan, indicating crosslinking had taken place. Up through 20 mol% XTA the observable BCB crosslinking temperatures fell between the degradation and melting temperatures of the copolymers. This indicated that melt processing of the copolymers was possible before inducing large amounts of crosslinking.

3.4. Thermal gravimetric analysis

The degradation temperature in nitrogen steadily decreased from 420°C as the XTA content increased. The 50% PET-co-XTA value was particularly low at 280°C, but this may be due to the low molecular weight of the 50% PET-co-XTA sample. Degradation in air occurred consistently at lower temperatures than in nitrogen, except for the 50% copolymer. In air degradation temperatures levelled

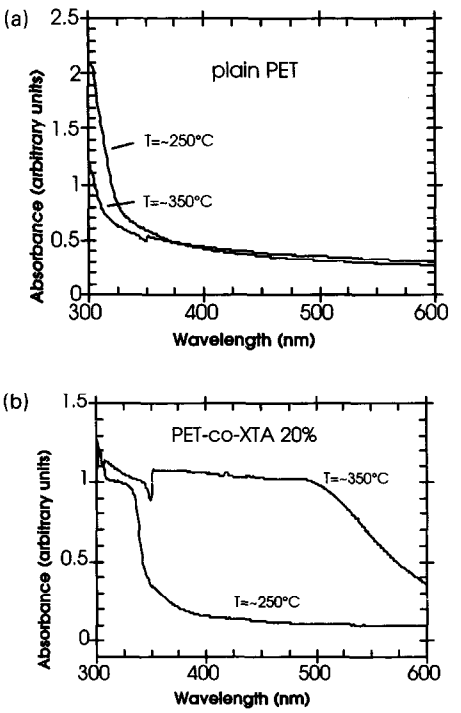

Fig. 6. Ultaviolet spectra for (a) neat PET; and (b) PET-co-XTA 20% heated to melt (250°C) and BCB-crosslinking (350°C) temperatures.

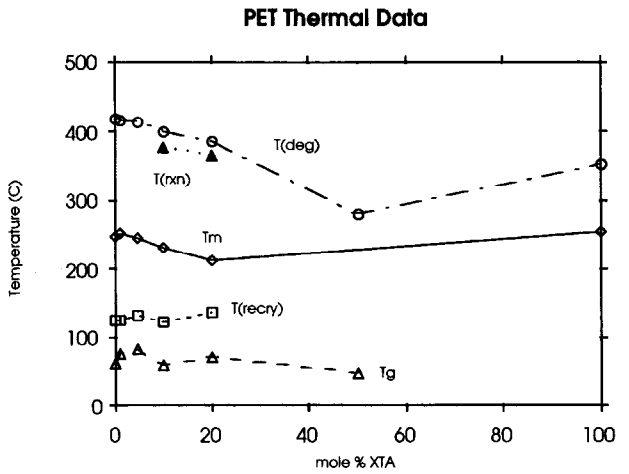

Fig. 7. Summary of the thermal data for the PET-co-XTA copolymers. The degradation temperature and melting temperatures steadily decreased with increasing XTA content, while the glass transition temperature increased slightly up to 5 mol% content of XTA, then decreased with increasing amounts of XTA. The BCB crosslinking temperature falls between the degradation and melting temperatures, leaving a processing window for the copolymers.

out or even increased for copolymers with 1–20% XTA, while in nitrogen they steadily decreased with XTA content. At 20 mol% XTA a 50°C, decrease was seen while at 100 mol% XTA the decrease dropped to about 70°C.

The decrease in degradation temperature associated with incorporation of XTA has been seen in other systems containing the BCB group. Marks and Sekinger noted a 60°C decrease in T_d in a 1:1 mol ratio BCB/BA copolymer compared with unmodified linear BPA PC [23]. Spilman reported a decrease of about 30°C in degradation temperature for PPTA-co-XTA copolymers on going from 1 and 25 mol% XTA, and a decrease of about 60°C was seen for PPXTA (the 100 mol% analog) [8]. Also, HBA/HNA-co-XTA copolymers showed a decrease in T_d with increasing XTA content [5]. The T_d of MPDI-co-XTA copolymers

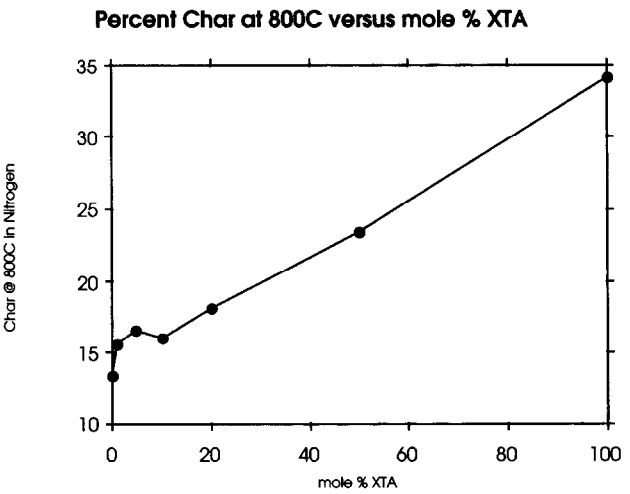

Fig. 8. The % char at 800°C versus the mol% XTA (in nitrogen). As the mol% XTA increases, there is a consistent increase in % char at 800°C. Neat PET had a % char of 13.4, while the PEXTA 100% had a % char of 34.1.

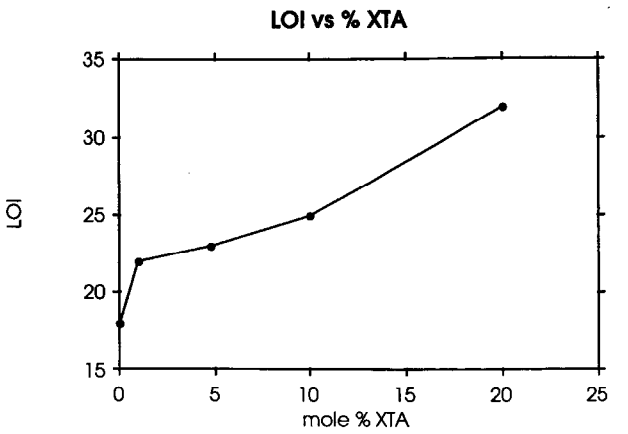

Fig. 9. Ignition resistance data for PET-co-XTA. As the XTA content increased, the LOI also increased. Neat PET had an LOI of 18, while the 20 mol% PET-co-XTA had an LOI of 32.

again decreased with increasing XTA, but the reduction was not as dramatic, from 1 to 50 mol% XTA only a 15°C drop was observed [8]. It is evident that adding the BCB group has generally decreased the thermal stability of most polymers studied to date. In some cases this may be from adding a relatively thermally unstable ethyl group to a relatively, thermally stable aromatic polymer (such as the PPTA and MPDI). Also, electron spin resonance (ESR) spectroscopy studies on PPXTA showed the generation of free radicals during heat treatment in the presence of oxygen [25]. An increase in free radicals was seen with time, indicating possible degradative chain scission. The proposed mechanism for crosslinking and subsequent degradation by free radical processes can be seen in Fig. 3. This process is probably significant in lowering the degradation temperature.

As the mol% of XTA increased there was a consistent increase in the % char at 800°C (Fig. 8). Plain PET had a 13.4% char while PEXTA 100% had a % char of 34.1. The char increased in a relatively linear rate with increasing XTA content except for some initial deviation at 1 and 5 mol% XTA.

3.5. Limiting oxygen index

Fig. 9 shows a plot of the LOI versus mol% XTA for the PET-co-XTA copolymers. The LOI steadily increased with increasing XTA content. The 10 and 20 mol% PET-co-XTA copolymers cracked extensively while coming out of the compression mold, causing some irregularities in LOI sample shape. All other test samples were uniform in size. The plain PET had an LOI of 18. When the PET burned the flame engulfed the entire sample and it dripped and melted. As the drips fell off they continued to burn until only char was left. The 1% PET-co-XTA had an LOI of 22. At a LOI of 20 and 21, the polymer started to drip, although this could have been pieces of char. The drip carried the flame off the sample then it went out. The 5% PET-co-XTA had an LOI

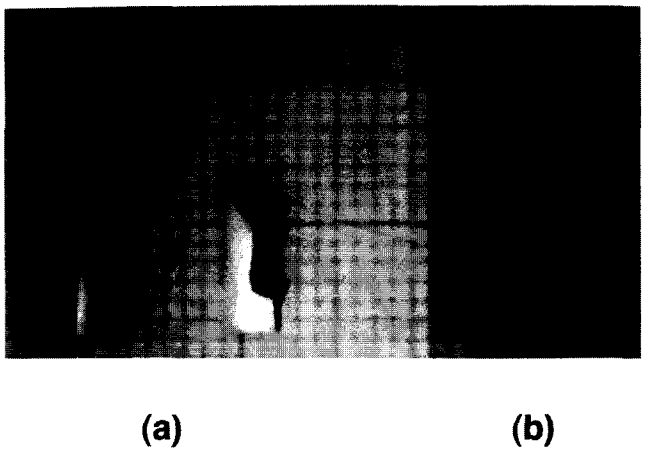

Fig. 10. Samples of (a) neat PET; and (b) PET-co-XTA 20% burned in air. While the neat PET burned with drips that propagated the flame PET-co-XTA 20% formed a thick char that terminated the flame.

of 23. In this case there were pieces of char which fell off carrying the flame, not drips. The 10% PET-co-XTA had an approximate LOI of 25. At this LOI the sample burned down the side, but not through the middle. Lighting it was also difficult, as some parts of the sample would light, but a flame which encompassed the entire sample was unachievable. The 20% PET-co-XTA had a LOI of 30–32. At an LOI of 27 and 29 the sample self-extinguished. When pieces of the polymer fell off carrying the flame, the outer layer burned until only a black char was seen, but underneath that initial char layer was fresh polymer. A visual comparison of similarly burned samples of neat PET and 20% PET-co-XTA is shown in Fig. 10, which clearly illustrates the difference in burning patterns between the polymer and copolymer.

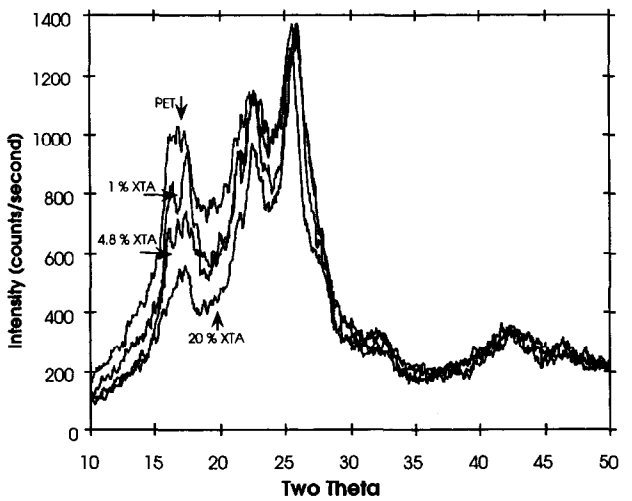

Fig. 11. PET and PET-co-XTA wide angle X-ray scattering data. The peak positions remain the same but decrease in peak intensity for copolymers with increasing XTA content.

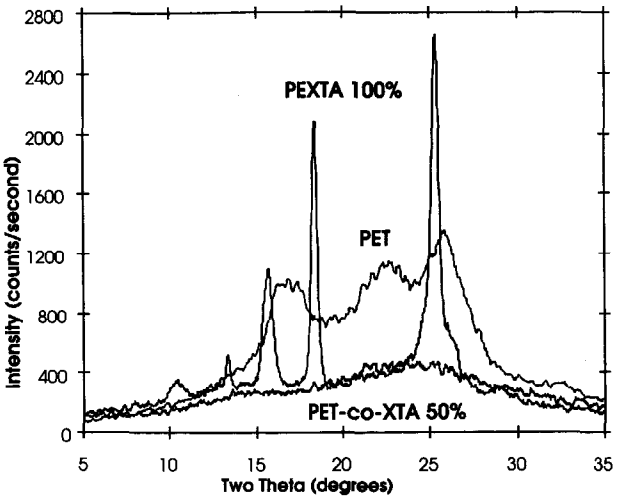

Fig. 12. WAXS data for neat PET, 50% PET-co-XTA and PEXTA 100%. The 50% PET-co-XTA showed little crystallinity. The change in two theta values for diffraction peaks for PEXTA relative to neat PET is indicative of a new crystalline structure.

3.6. X-ray diffraction

Fig. 11 shows a plot of the wide-angle X-ray scattering (WAXS) data for plain PET, as well for samples of PET-co-XTA. The crystal structure for PET is triclinic with $a = 0.456$ nm, $b = 0.595$ nm, $c = 1.075$ nm, $\alpha = 98.5°$, $\beta = 118°$, and $\gamma = 112°$. The space group for PET is $P\bar{1}$ [30]. The data showed only small differences between the X-ray patterns of plain PET and samples with low mol% of XTA, although the reduced peak intensity implied that the % crystallinity decreased with higher amounts of XTA. This suggested that at low mol% the XTA was not incorporated into the PET crystalline domains.

Fig. 12 compares the WAXS data for the higher mol% of PET-co-XTA with plain PET. At 50 mol% incorporation of XTA the WAXS pattern showed no diffraction peaks, indicating that the crystallinity was lost. The 100% PEXTA showed new diffraction peaks ($d = 5.86$, 5.64 and 3.54 Å) corresponding to the development of a different crystal structure. The sharpness of the peaks observed for the PEXTA 100% may be a symptom of the low molecular weight attained for this sample. Table 2 compares the d-spacings and two theta values for plain PET through 20 mol% PET-co-XTA to that of the PEXTA 100%.

WAXS data were taken after heat treatment of the PET and 20% PET-co-XTA for 30 min at temperatures from 250 to 400°C (Figs 13 and 14). The neat PET data showed a systematic decrease in crystallinity during degradation, while keeping the same relative d-spacings (Fig. 13). The 20% PET-co-XTA data also showed a decrease in crystallinity as the heat treatment progressed, but during intermediate temperatures new, relatively sharp Bragg reflections emerged (Fig. 14). The approximate d-spacings are 5.54, 5.07, 4.04, and 3.71 Å. These peaks evidently corresponded

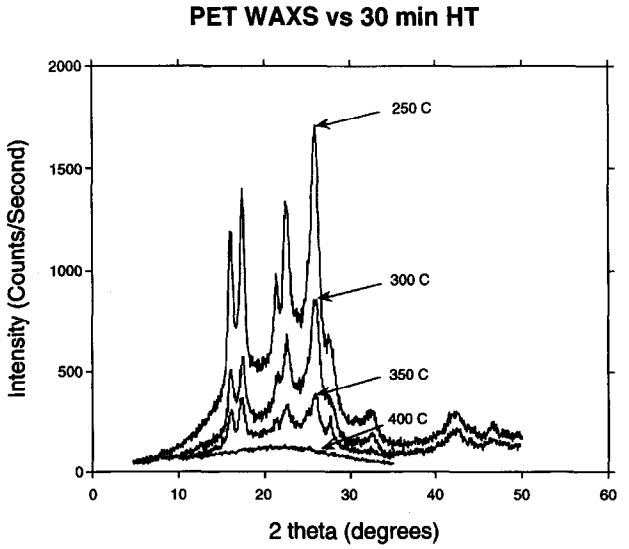

Fig. 13. WAXS scans for PET held for 30 min at temperatures from 250 to 400°C. The intensities of the Bragg peaks decrease in intensity with increasing heat treatment temperature, and there is no evidence for any new peaks formed at intermediate temperatures.

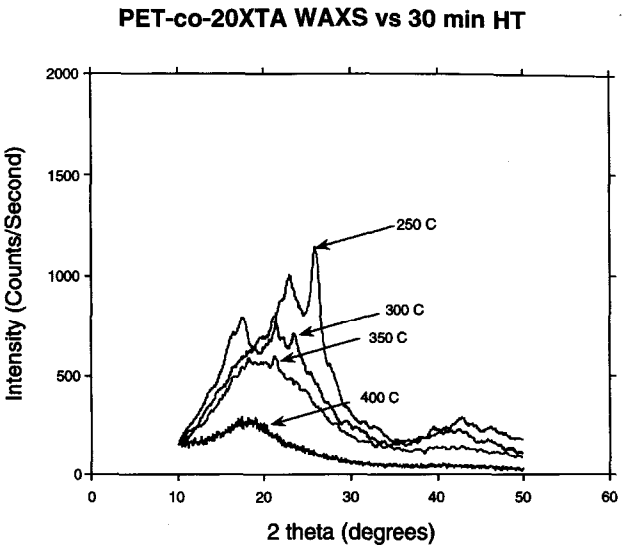

Fig. 14. WAXS scans for PET-co-20XTA held for 30 min at temperatures from 250 to 400°C. As for neat PET, the Bragg peaks decrease in intensity, but in this case there is now the development of new reflections at intermediate annealing temperatures. This corresponds with the development of a microcrystalline char layer formed near the surface, as seen in TEM.

to the development of a microcrystalline char layer, as was corroborated by transmission electron microscopy.

3.7. Transmission electron microscopy

The burned surface of the 10% XTA copolymer had a highly crystalline zone that was not evident in the PET homopolymer. As can be seen in the BF TEM images (Fig. 15), for PET-co-XTA 10%, this burned region contains dense particles with an average diameter of 300 Å. Within these particles were smaller crystallites as was confirmed by dark-field TEM images. The depth of the 'char' region was observed to vary in depth from 2 to 12 mm. Voids were also evident at the char-bulk interface. Below the interface, some voids could be also observed at what appeared to be interspherulitic boundaries.

In neat PET, the burned surface showed less obvious structural reorganization than in the PET-co-10XTA. However, thermal degradation was suggested by regions near the burn surface where the polymer failed under the physical stresses imparted by ultramicrotomy, forming a ribbon-like band of damage across the polymer. These regions penetrated to depths of ~0.1 mm. Dark-field images of neat PET did not show evidence of any increased crystallinity near the burn surface.

3.8. Fibre spinning

Fibres of the 0–20 mol% PET-co-XTA were successfully melt spun and examined with a Nikon optical microscope. There was little difference between the neat PET and PET-co-XTA fibres. Each fibre was about 50 microns in diameter. Very little birefringence was seen in any of the fibres under crossed polarized light. Each fibre was pulled to determine if the orientation could be increased. All of the fibres broke before significant drawing occurred, though each showed increased birefringence near the breaking point.

Table 2
Peak positions observed in wide angle X-ray scattering for PET and the PET-co-XTA copolymers

Neat PET through 20 mole% PET-co-XTA			PEXTA 100%	
2θ degrees	d-spacing Å	h,k,l	2θ degrees	d-spacing Å
16.29	5.43	0 $\bar{1}$ 1	15.1	5.86
17.37	5.10	0 1 0	15.7	5.64
21.57	4.11	$\bar{1}$ 1 1	25.1	3.54
22.68	3.92	1 $\bar{1}$ 0		
25.75	3.45	1 0 0		

Indices shown correspond to the known crystalline PET structure of Fu et al. (1993).

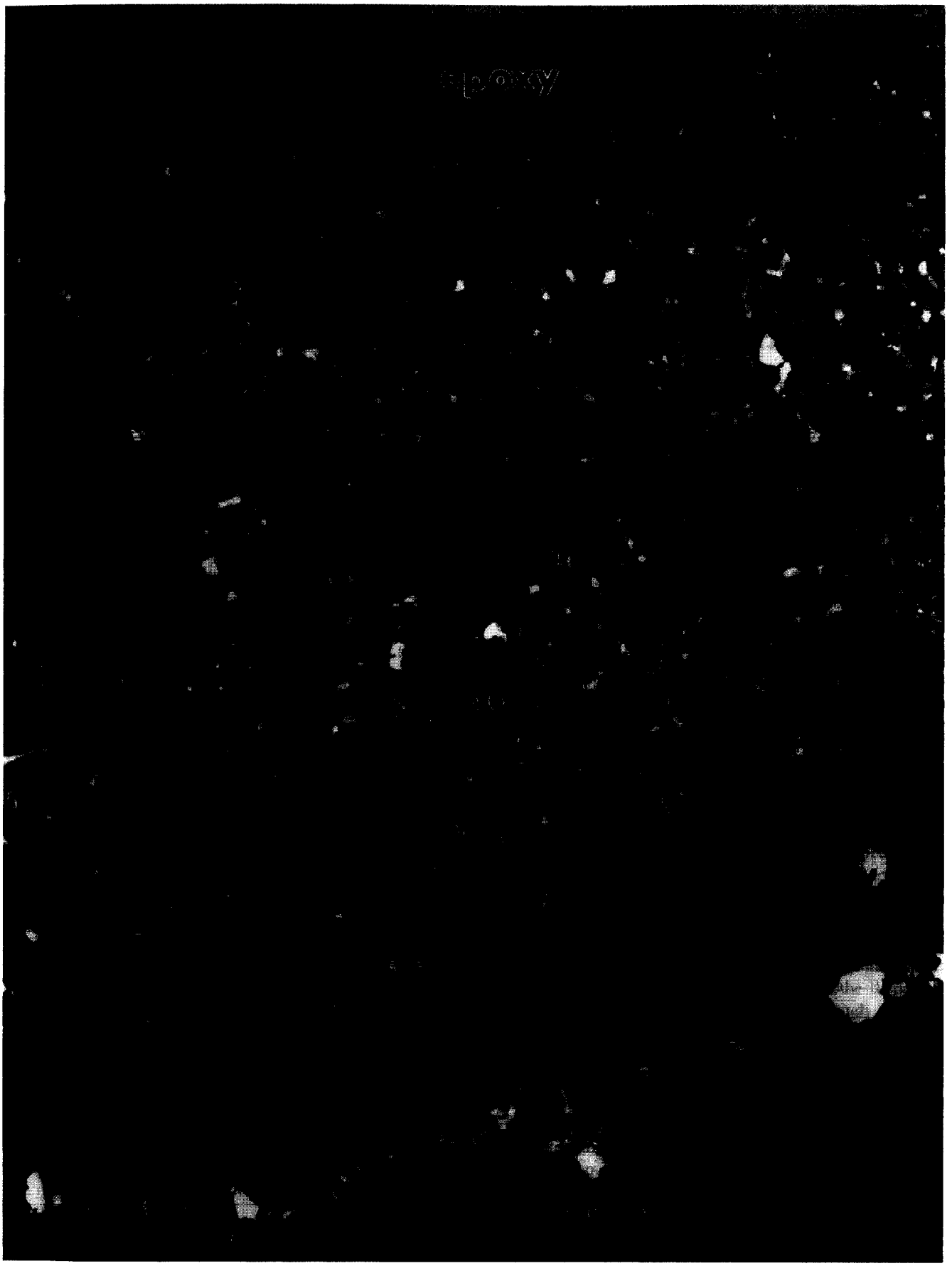
Epoxy

3.9. Adhesion

To assess the potential improvement in adhesion, samples of PET-co-XTA copolymer were heat treated while supported on a 125 micron thick PMDA-ODA (Kapton) polyimide film. After the neat PET was heated to about 400°C on the PMDA-ODA film it easily flaked off. This was not the case when the 20% PET-co-XTA copolymer was heated under identical conditions on the PMDA-ODA film. In this case the copolymer firmly adhered to the polyimide substrate. Attempts to remove it only caused the polyimde film itself to tear. This was compelling evidence that BCB crosslinking is a means of improving the adhesion performance of various polymers. Further work needs to be done to determine the overall effectiveness of this approach.

Mather and Romo-Uribe have investigated the complex viscosity of these copolymers as a function of temperature during heating at 10°C/min [31]. They observed that the neat PET and PET-co-1XTA materials both showed decreasing viscosities with increasing temperature. However, the viscosity of the PET-co-5XTA material was nearly invariant with temperature under these conditions, indicating that at this composition the rate of decrease of viscosity due to increased temperature was balanced by the increase in viscosity due to crosslinking. For 10% XTA there was a significant increase in viscosity, and for the 20% material this rise was even more dramatic. The profound influence of BCB crosslinking on copolymer melt rheology was clearly indicated by a nearly 5-fold order of magnitude increase in complex viscosity seen at elevated temperatures with the addition of 20% XTA [31].

4. Discussion

Our results demonstrate that it is possible to create PET-co-XTA copolymers with systematic variations in benzocyclobutene content. These functional copolymers show improved flame resistance and adhesion to polyimide substrates. They can be melt processed into fibres at intermediate temperatures. The BCB groups lead to enhanced flame resistance and char formation, which is particularly attractive given the all hydrocarbon structure of the functional group. The small size of the BCB moiety leads to only subtle variations in properties before the onset of the reaction, so that presumably other conventional PET processing schemes such as injection molding or blow molding could also be adapted for these new materials.

We have also obtained experimental evidence for increased adhesion between these BCB-functionalized PET copolymers and other polymer substrates. There is a decrease in the thermal degradation temperature of the polymers, although this effect is not as severe as has been seen for other high temperature-resistant materials. This is evidently due to the fact that the PET copolymers show a stable melt phase before thermal degradation. The increase in flame resistance appears to be that the crosslinking of the BCB units near the surface prevents further flow of material which propagates the flame. TEM micrographs show evidence for the formation of a microcrystalline char layer which evidently provides an insulating layer during burning. The detailed structure of these microcrystals remains to be established.

5. Conclusions

1. PET-co-XTA copolymers with controlled compositions can be synthesized by melt esterification to reasonable molecular weights. The synthetic technique requires more care than for neat PET to avoid crosslinking before obtaining high molecular weight polymer.
2. The PET-co-XTA copolymers show systematic variations in the glass transition, recrystallization, melting and degradation temperatures as a function of BCB content. The degradation and melting temperatures both decrease slightly with increased XTA, while the recrystallization and glass transition temperatures are relatively insensitive to XTA content.
3. The crosslinking temperatures (reaction onset ~350°C) fall below the degradation temperatures (~400°C) yet above the melting temperatures (~240°C), giving a processing window for the copolymers. This was confirmed by the ability to melt spin the PET-co-XTA samples into fibres.
4. LOI values for the copolymers systematically increased as the amount of XTA increased, from 19 for neat PET up to approx. 35 for PET-co-20% XTA. In addition, there was an almost linear increase in the % char at 800°C (in TGA analysis) as higher amounts of XTA were incorporated. Different burning characteristics were obvious between the neat PET and the PET-co-XTA. The PET melted and dripped while the PET-co-XTA formed a char layer which self-extinguished. The PET-co-XTA samples produced a significant amount of char compared with the neat PET samples.
5. X-ray scattering data suggest that XTA is excluded from PET crystalline domains which are able to crystallize well at XTA contents below 20%. The 50% copolymer showed little crystallinity, while the 100% PEXTA homopolymer developed a new crystalline structure.

Fig. 15. Bright field TEM micrograph of a microtomed cross-section of PET-co-10XTA copolymer near a surface that had been exposed to flame. There is a microcrystalline char layer which is readily distinguished from the bulk polymer and the epoxy embedding media. There is also evidence for void formation within the char and at the char–polymer interface.

6. WAXS showed the development of new d-spacings of the PET-co-XTA copolymers during annealing at elevated temperatures. TEM revealed the presence of a microcrystalline char region near the burn surfaces.
7. The PET-co-XTA copolymers demonstrated improved adhesion to polymer substrates after crosslinking.

Acknowledgements

This research was supported in part by the National Institute of Standards and Technology (NIST). The authors would like to thank Prof. Jeffrey S. Moore of the University of Illinois for technical assistance.

References

[1] Modern Plastics Magazine, McGraw-Hill, New York, 1997.
[2] Walker KA, Markoski LJ, Deeter GA, Spilman GE, Martin DC, Moore JS. Polymer 1994;35:5012–5017.
[3] Jones M-CG, Jiang T, Martin DC. Macromolecules 1994;27:6507–6514.
[4] Jiang T, Rigney J, Jones M-CG, Markoski LJ, Spilman GE, Mielewski DF, Martin DC. Macromolecules 1995;28:3301–3312.
[5] Mather PT, Chaffee KP, Romo-Uribe A, Spilman GE, Jiang T, Martin DC. Polymer 1997;38 (24):6009–6022.
[6] Walker KA, Markoski LJ, Moore JS. Synthesis 1992;12:1265–1268.
[7] Martin DC, Moore JS, Markoski LJ, Walker KA. US Patent No. 5,334,752, 1994.
[8] Spilman GE. Ph.D. Dissertation, The University of Michigan, 1996.
[9] The United States Fire Administration. Fire in the United States, 4th ed. Federal Emergency Management Agency, Washington, DC, 1982.
[10] Gann RG, Dipert RA, Drews MJ. In: Mark H, Bikales N, Overberger C, Kroschwitz JI, editors. Encyclopedia of polymer science and engineering. New York: Wiley, 1985.
[11] Nelson GL. Fire and polymers II. Washington, DC: American Chemical Society, 1995:2–26.
[12] Cullis CF, Hirschler MM. The Combustion of Organic Polymers. New York: Oxford University Press, 1981.
[13] Ebdon JR, Jones MS. In: Salamone JC, editor. polymeric materials encyclopedia, vol. 4. Boca Raton, FL: CRC Press, 1996:2397–2411.
[14] Kichhoff RA, Carriere CJ, Bruza KJ, Rondan NG, Sammler RL J. Macromol. Sci.-Chem. 1991;A28 (11) 12:1079–1113.
[15] Kirchoff RA, Bruza KJ. Adv. Polym. Sci. 1994;117:1.
[16] Farona MF. Prog. Polym. Sci. 1996;21:505–555.
[17] Deeken JS, Farona MF. J. Poly. Sci. A: Polym. Chem. 1993;31:2863–2867.
[18] DeLassus SL, Howell BA, Cummings CJ, Dais VA, Nelson RM, Priddy DB. Macromolecules 1994;27:1307–1312.
[19] Tan L-S, Arnold FE. J. Polymer Sci. A Polymer Chem. 1988;26:3103–3117.
[20] Tan L-S, Arnold FE. J. Polymer Sci. A Polymer Chem. 1988;26:1819–1834.
[21] Pabon RA Jr., DeVries RA. US Patent No. 5,310,809, 1994.
[22] Wong PK. US Patent No. 4,708,994, 1987.
[23] Marks MJ, Sekinger JK. Macromolecules 1994;27:4106–4113.
[24] Dang TD et al. Polymer Preprints 1995;36:455–456.
[25] Mielewski DF, Martin DC, Bauer DR. Proc. ACS Div. Polym. Mater.Sci. Eng. 1995;71:160.
[26] Walker KA, Markoski LJ, Moore JS. Macromolecules 1993;26:3713–3716.
[27] Wright CT, Paul DR. J. Membrane Sci. 1997; 129(1):47–53.
[28] Billica HR. US Patent No. 2,647,885, 1951.
[29] Lawton EL, Ringwald EL. In: Brandrup J, Immergut EH, editors. Polymer handbook, 3rd ed. New York: Wiley, 1989:V101–V105.
[30] Kilian VHG, Halboth H, Jenckel E. Kolloid-Zeitschrift 1960;172:166.
[31] Mather P, Romo-Uribe A. Polym. Eng. Sci. in press.
[32] Fu Y, Busing WR, Jin Y, Affholler KA, Wunderlich B. Macromolecules 1993;26:2187.